CONF-880122--17 EGG-M-38487

A MULTIMEGAWATT SPACE POWER SOURCE RADIATOR DESIGN

Jacek Jedruch 1/28/88

EBASCO Services, Inc.

Two World Trade Center

New York, NY, 10048

(212) 839-3283

EGG-M--38487

DE88 015185

INTRODUCTION

The multimegawatt space power sources (MMSPS) proposed for deployment in the late 1990s to meet mission burst power requirements, require an increase by four orders of magnitude in the power rating of equipment currently used in space. Prenger and Sullivan (1982) describe various radiator concepts proposed for such applications. They range from the innovative liquid droplet radiator (Mattick and Hertzberg 1981) to the more conventional heat pipe concept (Girrens 1982). The present paper deals with the design of the radiator for one such system, characterized by both high temperature and high pressure. It provides an estimate of the size, mass, and problems of orbiting such a radiator, based on the assumption that the next generation of heavy launch vehicle with 120-tonne carrying capacity, and 4000-m^3 cargo volume, will be available for putting hardware into orbit.

One of the concepts proposed to generate electrical power in the multimegawatt range in space in the 1990s is the liquid metal magnetohydrodynamic (LMMHD) energy conversion system, (Walker and Lake 1987), driven by a fast spectrum reactor. Operating with

DISCLAIMER

a Li coolant in the reactor core, it uses a foam of Li and He as the working fluid in the MHD energy conversion nozzle, and achieves all heat rejection from He passing through a radiator. The present paper deals with the heat rejection part of this energy conversion cycle, that is with the part of the system downstream from the inertial Li separators. It discusses the underlying considerations for proper sizing of the He radiator, and the philosophy guiding its conceptual design.

THERMODYNAMIC CONSIDERATIONS

The upper temperature of a nuclear heat source is a rule set by the ability of the construction materials to withstand their service conditions. Assuming that this temperature is fixed at maximum of 2350 K at the center of UN fuel rods, drops to 1500 K at the surface of W25Re fuel rod cladding, and is subsequently reduced to 688 K at the outlet from the MHD nozzles, the energy conversion efficiency of the present quasi-Ericsson closed cycle, can be further improved by lowering heat sink temperature.

In space applications of closed energy conversion cycles, heat rejection is restricted by necessity to radiation, and the fourth power law governing this process severely restricts the heat fluxes that can be accommodated at lower temperatures. This deficiency can be only compensated by increasing the radiator surface, and consequently, its mass. Therefore, the desire for higher efficiency of energy conversion must be traded off against the introduction of massive radiators required for heat rejection at lower temperatures.

In the present design, the radiator is divided into two sections, one servicing the intercooler between the two stages of the compressor, the other servicing the main system He coolant flow out of the inertial separators. For the main flow, the operating temperature range of the radiator was set between the limits of 688 K inlet and 420 K outlet, whereas for the intercooler, the temperature was set at 604 K inlet to 420 K outlet. The radiator outlet temperature selected above, is just below Li freezing temperature of 452 K. Although Li has very low vapor pressure (7.2 $\times 10^{-8}$ MPa at 688 K), traces of Li vapor will be present in the gas parts of the energy conversion system at all times. As it is desirable to inhibit plating out of Li in the radiator, the bulk of the radiator is designed to operate at temperatures above the 450 K freezing temperature of Li.

SOLAR HEATING EFFECTS

Solar energy flux deposits on the surface of the radiator 1.37 kW/m^2 of radiant energy, or 13.7 MW per hectare of radiator surface. This constitutes a significant power input for a radiator in the standby or alert mode. In the power burst mode, the solar heat flux contribution to the radiator heat load is not significant. As these figures indicate, the question of radiator orientation relative to the sun should be included in the operation plan of the MMSPS in its dormant and alert modes. From the point of view of minimizing solar heating of the radiator, one of the more compact configurations discussed below, is more efficient than a simple planar radiator.

Should the MMSPS be placed in a geostationary orbit, the solar heating effect contributes an oscillating heat load, superimposed on the base load resulting from the regular reactor operation in the standby, alert and the burst modes. In the first of these, it will become a significant part of total load, contributing to the thermal stress in the structure. Design of the joints between the panels must make provisions for these variable loads.

SELECTION OF OVERALL GEOMETRY

An overriding consideration present with all radiators serving a space nuclear reactor heat source is the necessity to orient the radiator such that it presents minimum area facing the reactor. With this orientation, the amount of additional heat deposited in the radiator material by interaction of its structure with gamma and neutron radiation emitted from the reactor is minimized.

The radiator edge closest to the reactor, receives the highest heat load, and the gamma and neutron heat load falls off with inverse square of the distance separating any radiator point from the reactor, plus any self-shielding for the parts of the radiator further away by the material of the radiator itself. For large reactor powers, the size of the radiator is much larger than the reactor, so that to a first approximation, the reactor can be considered point source of radiation. Effects of nuclear radiation shield interposed between the reactor and the radiator, appear as angular perturbations to the otherwise spherical distribution of the emitted radiation. In the absence of significant atmosphere, the effects of skyshine are virtually eliminated, and cause the radiation field contributing to the radiator heat load to take the form of line-of-sight configuration.

Three basic geometrical shapes were considered in selection of the gross radiator configuration for the LMMHD system: 1) frustum of a cone, 2) rectangular plane, 3) 3-D cruciform. Each of them can be arranged such, that it faces the reactor on edge. Superimposed on this overall shape is the fine structure of the radiator surface dictated by the subdivision of the radiator into panels, of size suitable for transport into space, by the provisions for gas manifolds, plus the valving, and tubing of the actual radiator surface.

Of the three basic configurations listed above, the performance of radiators configured in a frustum of a cone is best documented, having been selected in the past for use in the SNAP series, and again for the SP-100 reactor. It provides a relatively compact radiator, which could be mounted on the heat source prior to launch into space, and for power sources rated in the kW range, it would fit into the bay of the space shuttle. This consideration overrides the obvious disadvantage of this configuration, namely that only the outside of the cone radiator has an unobstructed view of space. The inside of the cone radiates partially to itself. For power ratings in the MW range, the fully assembled conical radiator does not fit into the bay of the space shuttle and parts of it must be folded on themselves for launch, and be unfolded in space. For power ratings in the 10s to 100s MW range, the conical configuration of the radiator offers no advantage, since it requires disassembly for launch, and reassembly in space is more complex.

A rectangular planar radiator has the largest overall dimensions, and thus requires longest manifold piping. It also is most sensitive to solar heating, unless kept oriented on edge to the sun at all times. For some orbits, this may require an active program of continuous reorientation with respect to sun, a troublesome, and energy consuming process. Thus, even though conceptually simple, the planar radiator is not the best choice of configuration.

After the elimination of the conical and the planar configurations, a cruciform configuration was chosen for the radiator, with its wings oriented on edge to the axis connecting the reactor with the payload platform, see Figure 1. Each of the four wings was divided into panels 10 m by 40 m in dimension. Part of each wing, the two panels closest to the radiator axis and to the reactor, were reserved for mounting on them the energy conversion equipment, such as the pumps, MHD nozzles, inertial separators, and compressors.

The remainder of each of the four radiator wings is divided into four rows of panels, each row separated from the succeeding row by outlet headers, feeding into inlet headers through spring loaded check valves, see Figure 2. These valves are designed to isolate any panel, decompressing as a result of meteorite, or other damage. This configuration of the radiator, backed up by a panel isolation feature, allows sacrificing part of the radiator in the event of panel damage, without loss of the entire radiator wing. Thus, redundancy in radiator surface is substituted for maintainability.

SELECTION OF RADIATOR MATERIALS

The construction material for the piping, headers and valves must be a light, high strength alloy, compatible with Li vapor, and retaining sufficient strength in the temperature range considered for this design. After a survey of the available materials, Ti-6Al-4V alloy was selected. This alloy has a density of 4.43 g/cc, with yield stress of 414 MPa at 800 K. The radiator tube ID is 5.17 cm, chosen to produce a reasonable pressure drop in the 40 m long panels. For a design safety factor of 2, a wall thickness of 0.0367 cm is required to contain He at 3.0 MPa internal pressure. This thickness was rounded off to 0.04 cm for our purposes. The radiator tubes are separated by flat Al fins, of width and thickness determined through an optimization described below. The radiator tubes and fins are coated on the outside with calcium titanate, which has emissivity of 0.89 and good bonding capability. Initially, a Be meteorite shield layer was considered for an intermediate layer between the tube material and the coating. Wossner (1973) indicates that at least 0.269 g/cm^2 areal density of Be (1.5 mm at 1.795 g/cc) is required to be effective, i.e. approximately 1.5 times the areal density of the tube material itself of 0.177 g/cm^2. Addition of this meteorite protection will more than double the radiator mass. For this reason, a sacrificial redundant area of radiator, rather than increased radiator tube thickness was chosen for this design, recognising the fact that it is impossible to completely shield against punctures inflicted by meteorites or space debris.

METHOD OF ANALYSIS

Three aspects of radiator design were the subject of particular attention:

1) selection of radiator surface (the spacing of tubes and the thickness of fins separating them),

2) proportions of the cruciform leaves of the radiator (length to width ratio in relation to the radiation view factors),

3) distribution of He temperature in passage through four successive panels in the radiator.

To handle these problems, the method of analysis suggested by Wossner (1973), Sparrow and Jonsson (1963), Sparrow and Cess (1966) and Rohsenow and Hartnett (1966), was used. In particular, the following equation was used to calculate the tube-to-tube view factor with intervening partition:

$$F_{1-2} = \frac{1}{\pi}\left[0.5\,\pi - (2\Omega - 1) + 2\sqrt{(\Omega^2 - \Omega)} - \arccos\left(\frac{1}{2\Omega - 1}\right)\right]$$

where:

$\Omega = 1 + \frac{L}{R}$ the ratio of half fin width to tube radius, see Fig. 3

Power per unit area of the radiator (W/cm^2) was computed from:

$$\frac{q}{A} = (1 - 2\,F_{1-2})\,\epsilon\,\sigma\,T^4$$

where :

$\sigma = 5.67 \times 10{-}12\ W/cm^2\,K^4$ is the Stefan constant.

To compute the heat conduction from the tubes into the fins separating them, the analysis was done in terms of the design parameter N_C :

$$N_C = \frac{\epsilon\,\sigma\,T^3}{k} \times \frac{L^2}{t}$$

where L, t are fin half width and half thickness, respectively and k = 1.6 W/cm K is the thermal conductivity of Al fins.

The expression for the computation of radiator area was obtained from the integration of the point power equation:

$$A = \frac{q}{\epsilon\,\sigma\,(T_H - T_L)} \times \int_{T_L}^{T_H} \left(\frac{dT}{T^4 - T_S^4}\right)$$

where: T_H, T_L - high, low temperature of heat rejection (K)

T_S - heat sink temperature (K)

Since $T_S^4 \ll T_L^4$, this expression becomes:

$$A = \frac{q}{3 \epsilon \sigma (T_H - T_L)} \times \left(\frac{1}{T_L^3} - \frac{1}{T_H^3} \right)$$

whereas, the mean emission temperature is: -

$$\bar{T}^4 = 3 \, (T_H - T_L) \times \frac{T_H^3 \times T_L^3}{T_H^3 - T_L^3}$$

RESULTS OF DESIGN OPTIMIZATION

Fin thicknesses (2t) varying from 0.3 to 0.13 cm, fin widths (2L) from 4 to 16 cm, and the radiator surface temperatures from 360 to 850 K were considered for this concept, and a central composite orthogonal design in the three variables was set up, relating to them power per unit mass of the radiator. The resulting expression was as follows:

$$P/M(W/g) =$$

$$6.5922 + 8.5227 \times 10^{-2} L + 1.4377 \times 10^{2} t - 4.7704 \times 10^{-2} T$$
$$-2.0237 \times 10^{-2} L^2 + 4.9439 \times 10^{2} t^2 + 7.077 \times 10^{-5} T^2$$
$$-1.1516 \times 10^{1} Lt + 1.4272 \times 10^{-3} LT - 3.1812 \times 10^{-1} tT$$

The plot of this response surface is shown in Figure 4. It shows the area power density of the radiator to be a very weak function of fin half width and fin half thickness, a very strong function of radiator surface temperature. On the basis of this the fin width of 15.24 cm with fin thickness of 0.4 cm (the same as the tube thickness) is specified for the first three panels from the inlet to the radiator, whereas a tube spacing of 5.08, combined with 0.16 cm fin thickness is specified for the last panel at the radiator outlet. At the larger tube spacing, 49 He tubes are placed in one 10 m wide panel. To provide a degree of stiffness, not possible with the 0.04 cm thick fins, stiffening ribs are placed 5 m apart along the 40 m length of the panel.

The panels in each wing serve as both the main radiator and the intercooler radiator, but are connected to a separate header sys— tems for a total of 416 panel for both radiators. This number contains an allowance for the cross-talk between the wings, in the cruciform arrangement of the radiator. Figure 5 shows the fraction of power radiated to space as a function of wing length to wing width ratio a/b and c/b. Assuming identical wings, with a/b = c/b = 1.66, the fraction of power radiated into space is 0.825, while 0.175 is absorbed by the panels in the other wings. This loss is the price of compact radiator design.

CONCLUSIONS

The effective areal power output for both sides of the radaitor, including tube and wing cross-talk factors, is: q/A=4.92 kWt/m^2. The radiating surface alone is estimated to have the mass of 257 tonnes. This increases to 600 tonnes when the headers, valves, panel stiffener are included. This corresponds to 0.78 kg/kWt. The volume of the radiator, when the panels are folded accordion-like, is 8317 m^3. If headers of 2.5 times the diameter of the radiator tubes are used, the folded radiator volume rises to 20,792 m^3.

These numbers are more meaningful relative to the load carrying capacity of the conceptual super-shuttle, assumed to have a 120 tonne, 4000 m^3 cargo bay. Approximately 5 shuttle loads will be required to bring the radiator components into orbit, admittedly, the most bulky part of the system. Additional shuttle trips will be required to bring the reactor and the energy conversion equipment into orbit. The significance of these estimates is that multiple launches, assembly in space, and markedly increased cargo carrying capacity of the space shuttle will be required for orbiting space sources of this magnitude.

Acknowledgments

The work described here was partially supported by U S Department of Energy Contract No. DE-AC07-76ID01570 with Idaho National Eengineering Lab., and INEL's Subcontract No. C85-100796 with Ebasco. The author wishes to thank Dr. R. L. Hensler for helpful suggestions regarding analytical methods.

References

J. R. Bilton, R. Hensler, V. Walker, B. Rushton, R. Ambrosek, B. Schnitzler, F. Wheeler, V. Storhok, J. Lake, R. Wadkins (1987), "A Liquid Metal MHD Concept for Multimegawatt Space Power Application," 4th Symp. Space Nucl. Power Sys., Albuquerque, NM, Jan. 12-16, 1987, pp. 411-414.

S. P. Girrens (1982), "Design and Development of a Titanium Heat Pipe Space Radiator," Los Alamos National Laboratory, LA-9251-MS, March 1982.

A. T. Mattick and A. Hertzberg (1981), "Liquid Droplet Radiators for Heat Rejection in Space," J. Energy, AIAA 80-9477R, Nov.

1981, pp. 268-69.

F. C. Prenger and J. A. Sullivan (1982), "Conceptual Designs for 150-MW Space Radiators," NAS Symp. Adv. Concept Reactors, Washington, DC, 15-17 Nov. 1982.

E. M. Sparrow, V. K. Jonsson (1963), "Angle Factors for Radiant Interchange Between Parallel-Oriented Tubes," Trans. ASME, J. Heat Transfer, Nov. 1963, pp. 382-384.

E. M. Sparrow, R. D. Cess (1966), "Radiation Heat Transfer," Brooks/Cole Publishing Company, Belmont, CA, 1966., pp. 170-176.

W. H. Rohsenow, J. P. Hartnett (1973), "Handbook of Heat Transfer", McGraw-Hill Book Co., New York, 1973, Ch. 15.

G. Wossner (1973), "Optimization of Plane Fin-Tube Radiator for Spacecraft Energy Supply," NASA TT F-16473, Washington, DC, Aug. 1973.

FIGURE 1
OVERALL RADIATOR LAYOUT

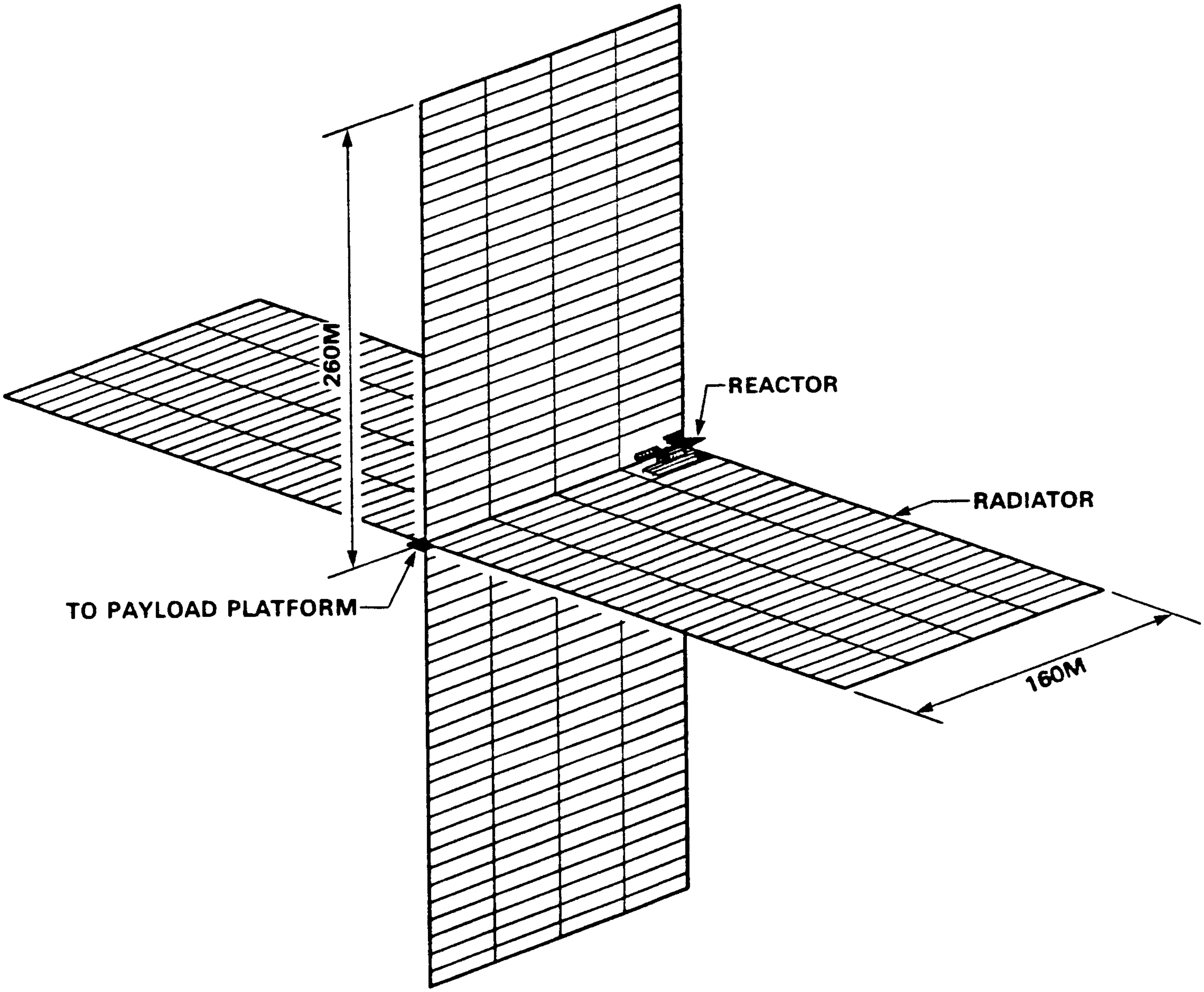

FIGURE 2. PANEL LAYOUT

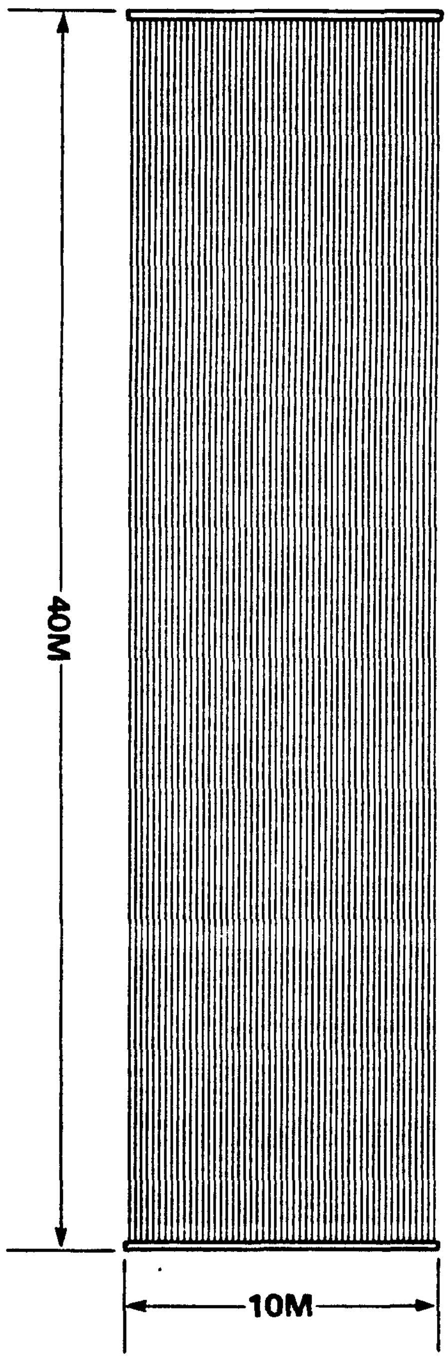

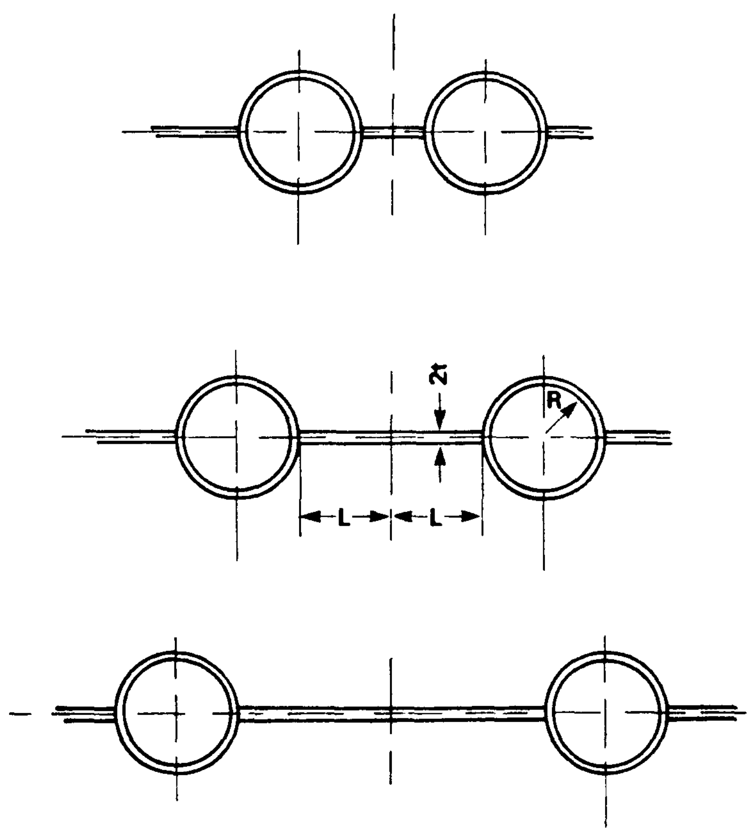

FIGURE 3
THREE TUBE GEOMETRIES

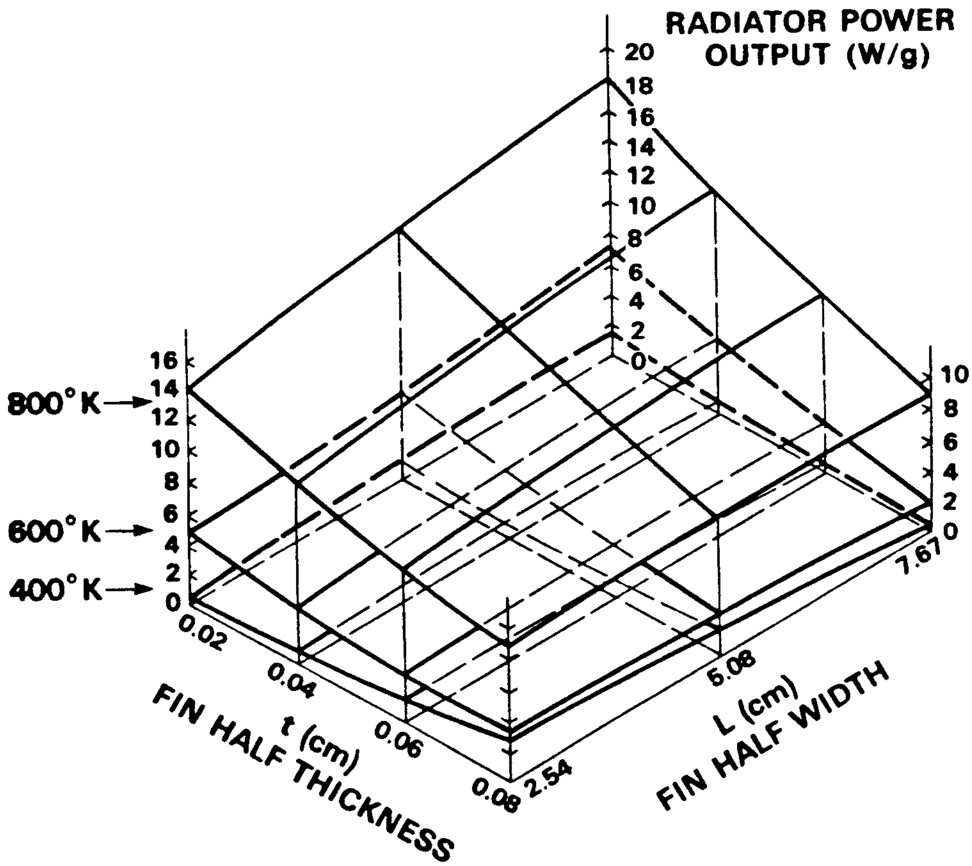

FIGURE 4
RADIATOR POWER VS. TEMPERATURE AND FIN DIMENSIONS

FIGURE 5
POWER DISSIPATED VS. ASPECT RATIO

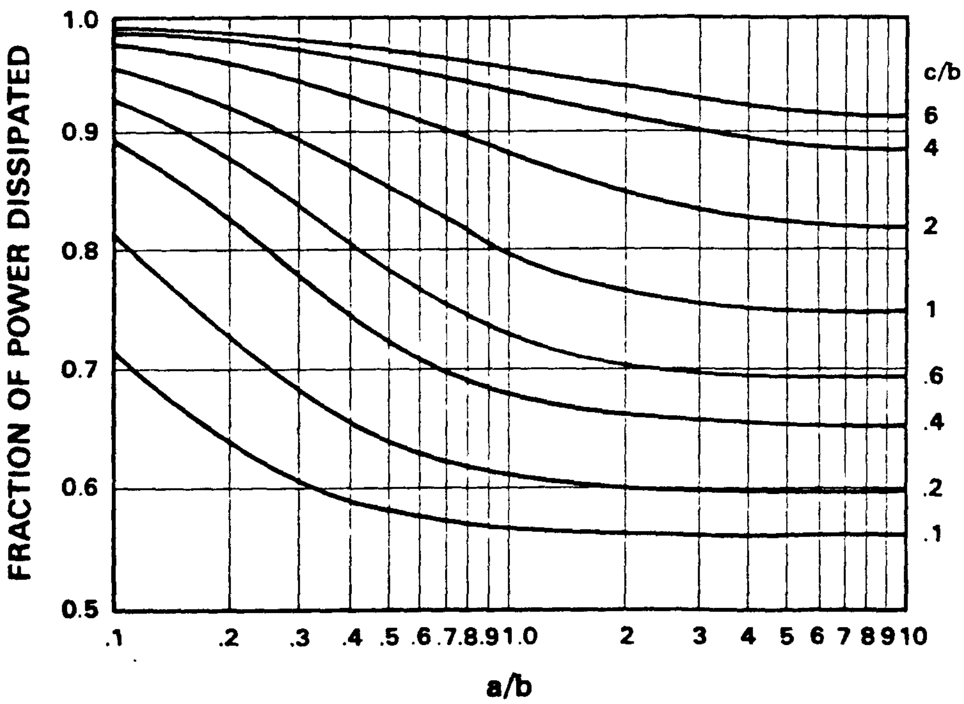

DISCLAIMER